EMG-Based Decoding of Manipulation Motions in Virtual Reality: Towards Immersive Interfaces

Anany Dwivedi, Yongje Kwon, and Minas Liarokapis

***Abstract*— To facilitate the development of a new generation of Virtual Reality systems and their introduction in everyday life applications, new intuitive, immersive methods of interfacing have to be developed. Over the years, Electromyography (EMG) based interfaces have been utilized for unobtrusive interaction with computer systems. However, previous EMG studies have not explored the continuous decoding of the effects of human motion (e.g., manipulated object behavior) in simulated and virtual environments. In this work, we present an EMG based learning framework that can allow for an immersive interaction with Virtual Reality environments. To do that, EMG activations from the muscles of the forearm and the hand were acquired during the execution of object manipulation tasks in a virtual world along with the motion of the object. The virtual world was visualized using an HTC Vive VR headset, while the hand motions were tracked with a dataglove equipped with magnetic motion capture sensors. The object motion decoding was formulated as a regression problem using the Random Forests methodology. The study shows that the object motion can be successfully decoded using the EMG activations, despite the lack of haptic feedback.**

I. Introduction

Over the years, an increasing number of applications in entertainment, medicine, retail, research, and education has utilized Virtual Reality (VR) and Augmented Reality (AR) systems. VR based games have a positive impact in healthcare, as such games can be used in motion rehabilitation in stroke patients [1]. In [2], authors employ a VR based immersive environment for the study of neuronal tissues for exploring local cellular interactions. In [3], the authors presented the effectiveness of VR / AR systems in education and concluded that they result in increased engagement of the learner.

Traditional methods of interaction with such systems include hand-held controllers and speech and/or vision based gesture recognition devices. But the use of buttons, joysticks, track-pads, or triggers for interaction with a dynamic and unstructured environment is less intuitive when compared to the use of one's arms and hands. In [4], the authors quantitatively present that using hand gestures directly results in improved embodiment than using controllers. A few other drawbacks of the traditional methods of interfacing are: i) they utilize bulky hand-held controllers that are inadequate for intuitive and non-fatiguing interaction with the system [5], ii) the vision based systems are prone to occlusions [6], and iii) speech and vision based systems depend on environmental factors like ambient light and background noise. Moreover, these interfaces capture only the kinematic information of the gesture performed by the user and not the effort put in by the user. Due to these issues, there is a need for an intuitive interfacing method that can provide an embodied interaction with dynamic and unstructured environments.

Anany Dwivedi, Yongje Kwon, and Minas Liarokapis are with the New Dexterity research group, Department of Mechanical Engineering, Faculty of Engineering, The University of Auckland, New Zealand. E-mails: adwi592@aucklanduni.ac.nz, ykwo675@aucklanduni.ac.nz, minas.liarokapis@auckland.ac.nz

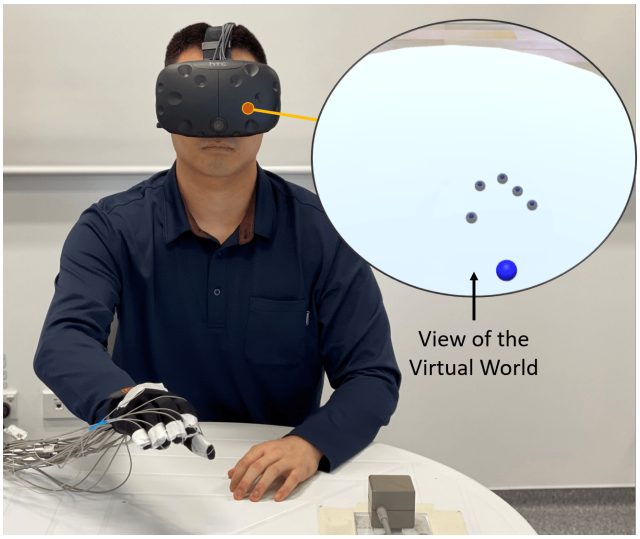

Fig. 1. User interacting with the virtual environment. The HTC Vive VR headset is used to visualize the virtual world, while the hand positions and orientations are tracked using a dataglove equipped with a magnetic motion capture system. EMG activations are acquired during the experiments. The inset figure shows the user's view of the virtual world.

Most of the above mentioned issues can be addressed by using Muscle Computer Interfaces (MuCIs). MuCIs decode human intentions by utilizing myoelectric activations and allow for an immersive interaction with various devices. In [6], authors present an interfacing scheme that is capable of decoding the task performed by the user even when hands are under load. In [7], authors presented an unobtrusive arm band that consists of electromyography (EMG) sensors placed on the forearm. Moreover, EMG based interfaces being hands-free allow for a more natural control of interaction with different devices, which makes them an appropriate, intuitive method for teleoperation applications with robot arm-hand systems [8]. Past studies have focused on EMG based decoding of reach to grasp motions [9], [10] and execution of various types of grasps [11] and finger movements [12]. These interfaces have also been successfully used for teleoperation of robotic arm-hand systems [13], games [14], wearable MuCIs, and even interaction with virtual environments. In [15], Berger et al. proposed

a framework that used a VR system with an EMG based interface. They performed analysis on arm movements by studying their muscle synergies. Such analysis can be used to provide an insight enhancing the rehabilitation process for individuals with impaired motor functions. However, there is a lack of studies focusing on decoding complex motions, such as equilibrium point manipulation of an object (where the contact points remain stationary), in a virtual world. Developing systems that decode such complex motions can be used to enrich the immersive experience in VR.

Previously, we proposed a learning scheme that decodes real object motions from the myoelectric activations of the muscles of the forearm and the hand [16], [17] and explored the effects of gender and hand sizes on the performance of decoding the object motion [18]. We also studied the differences of in-hand manipulation motions of real objects that had centered and off-centered mass [19]. In this work, we propose a learning framework that can enable immersive interactions with VR systems utilizing EMG based decoding of dexterous, in-hand manipulation motions. To do this, we employ appropriate Random Forests regression models that decode continuous object motions of manipulation tasks executed in a virtual world (see Fig. 1). This study shows that it is feasible to decode virtual object motions using just the EMG activations of forearm and hand muscles, without the presence of haptic feedback and without accounting for other dynamic phenomena such as friction, rolling, or slipping.

The rest of the paper is organized as follows: Section II describes the equipment used and the experiments conducted, Section III describes the proposed learning scheme, Section IV presents the results, while Section V concludes the paper.

II. Apparatus and Experiments

The experiments were performed by 5 able-bodied male subjects with their dominant hand (age = 26 ± 1, hand length = 186 ± 15 mm). Two subjects were left hand dominant while three subjects were right hand dominant. The study has received the approval of the University of Auckland Human Participants Ethics Committee (UAHPEC) with the reference number #019043. Prior to the study all subjects provided written and informed consent to the experimental procedures.

A. Experimental Setup

In the experiments the subjects were required to perform manipulation tasks in a virtual environment (see Fig. 2 for the virtual objects used in the experiments). To enable these interactions, HTC Vive was selected as the VR system while the Polhemus Liberty motion capture system was used to track the finger motions. The virtual world was rendered in Unity and the real world physics was modeled using MuJoCo. To track the positions and orientations of the hand, subjects wore a dataglove equipped with six magnetic motion capture micro-sensors that were connected to the Liberty system. Five sensors were placed on each of the five fingertips, while one sensor was placed at the back of the palm. The EMG signals were acquired using g.Tec's g.USBamp bioamplifiers.

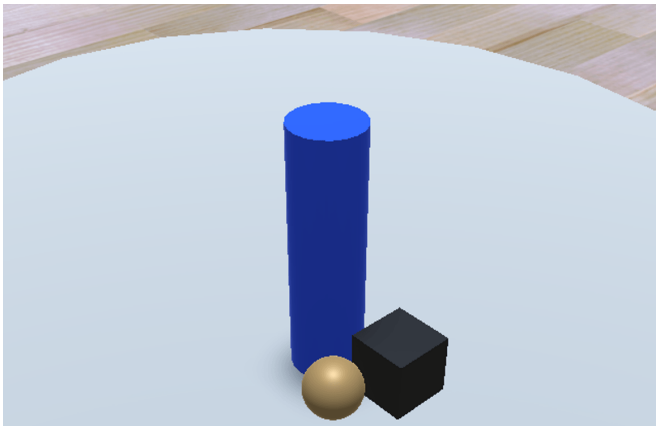

Fig. 2. The object set used in the virtual world. The set includes a cube, a cylinder, and a sphere.

The physical setup for the virtual world experiments included a chair and a table for the subject to sit and perform the experiments. It was made sure that this area was in the field of view of the HTC Vive's base stations for the tracking of the head motion and orientations. The virtual world consisted of a table that was closely designed and positioned to match the table in the real world. The objects were positioned on this table for the user to grasp and perform the manipulation experiments. The objects used in the experiment were a cube, a cylinder, and a sphere and they were modelled based on the objects available in the YCB object set [20]. Fig. 3 shows the experiment setup in the real and virtual worlds.

B. Physics Simulation Setup

To simulate and visualize the virtual world, MuJoCo and Unity were utilized. MuJoCo is a physics engine developed by Todorov et al. [21] known for its fast and accurate physics simulations. It was used to simulate the dynamics of the virtual hand and the objects, using the tracked finger positions from the motion capture system. Unity was used to interface the liberty motion capture system and MuJoCo, and also to render, display, and record the positions and orientations of bodies generated by MuJoCo. It should be noted that physical parameters of the environment affect the motion of the bodies, such as, the air density affects the lift and drag forces of moving bodies, whilst the viscosity affects the viscous forces of moving bodies. So in MuJoCo, the environment was setup so that the environmental conditions were similar to those of Earth (e.g. gravitational acceleration, air density, and viscosity were set to -9.81 m/s^2, 1.2 kg/m^3 and 20 μPas respectively).

The manipulation motions were executed only on virtual objects without handling a real object in the hand. Due to this, a direct tracking of the object motion was not feasible. So, the position and the orientation of the grasped object were tracked by calculating the forces exerted by the fingertips of the subject on the object. The proposed approach uses two bodies for each fingertip (See Fig. 4). One body, the motion body, follows the position of the fingertips tracked by

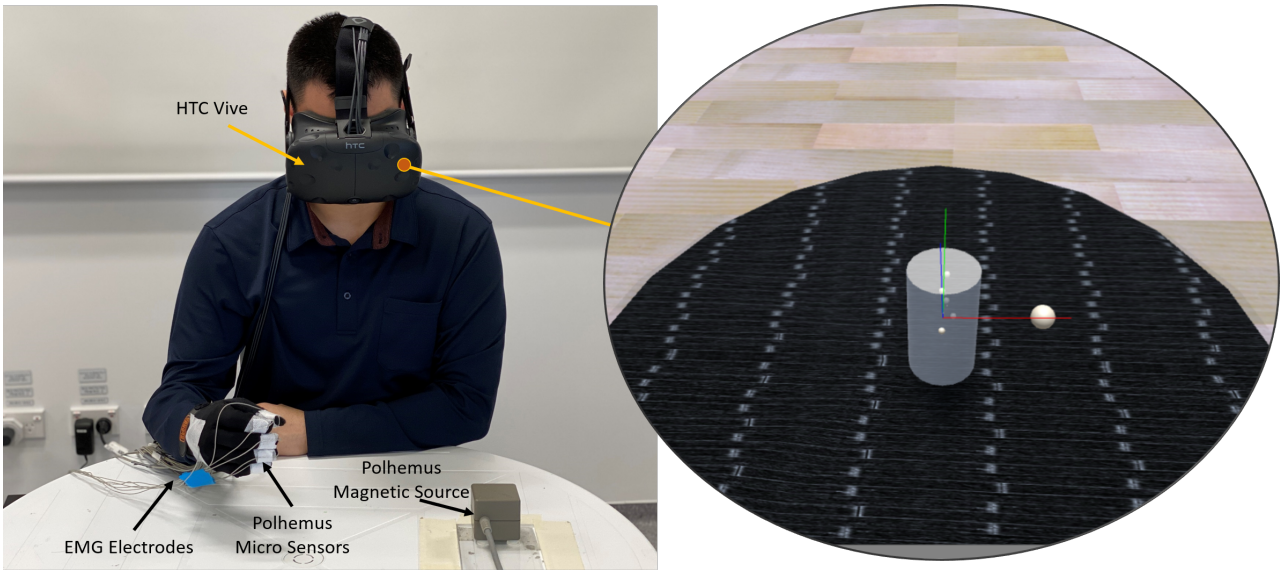

Fig. 3. Setup of the experiments conducted in this study. This figure shows a virtual cylinder being dexterously manipulated by a right hand dominant subject. The subject is shown wearing the HTC Vive VR headset and has EMG electrodes attached to their dominant hand that record the myoelectric activity of the muscles during manipulation of the virtual object. A glove equipped with Polhemus magnetic motion capture micro-sensors that track finger motion is used. The inset figure shows the view of the virtual world being displayed on the headset worn by the subject.

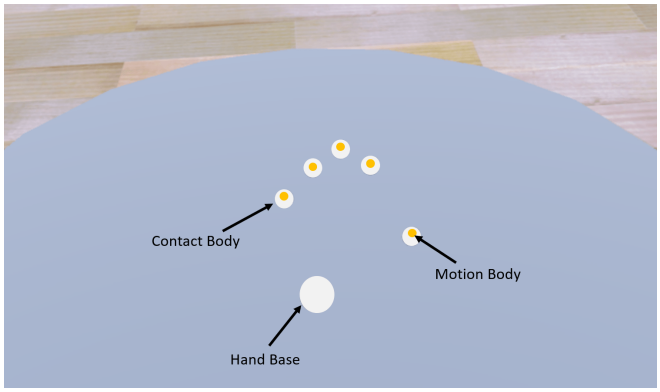

Fig. 4. Representation of a human right hand in the virtual world. The hand base represents the palm of the hand while the motion and contact bodies represent the fingers and the thumb. The palm of the hand is looking upwards. The contact body is used to make and detect contact with the objects while the motion body is used to project the position of the subject's hand in the virtual world. The contact body is constrained to follow the motion body and once there is contact with the object, the force that each contact body exerts on the object is determined by the distance between the motion body and the contact body.

the motion capture system, but it does not make contact with the virtual object. The other body, the contact body, is constrained to follow the motion body until it collides with the surface of the object where it can no longer follow the motion body if it has entered inside the object. If such a collision occurs, the simulation can produce a force proportional to the distance between the bodies on the object, which causes the object to move. By doing so, this prevents interpenetration of bodies in motion, which is an unwanted condition of physics engines as the bodies produce abnormally large forces to separate away from each other, resulting in unstable simulations. Moreover, the contact dynamics were setup to minimize contact rolling because the manipulation motions involved in these experiments required the contact points of the fingers to be relatively stationary on the object surface. To do this, the friction forces tangential to the object were chosen so as to strongly oppose slip during manipulation. All these considerations led to the selection of appropriate object manipulation physics in the virtual environment that closely resemble the physics of the real world.

C. Muscle Selection

To decode the motion of the virtual objects during the execution of the dexterous, in-hand manipulation tasks, the myoelectric activations of the human forearm and the hand were recorded. The muscles of the hand include the lumbricals, opponens pollicis, dorsal interrosei, and opponens digiti minimi. The muscles of the forearm include the flexor digitorum superficialis, extensor digitorum superficialis, and the abductor pollicis longus (see Fig. 5). For the experiments, the g.Tec's g.USBamp bioamplifier was used. The settings of the bioamplifier that were configured for these experiments included a sampling rate of 1200 Hz, a Butterworth bandpass filter with cutoffs 5 Hz and 500 Hz, and a notch filter of 50 Hz to attenuate the line noise.

D. Experimental Tasks

Before the start of the experiments the subjects were given verbal and visual instructions about the experiment tasks. The experiments consisted of executions of three different manipulation tasks on three virtual objects. The experiments were divided into three different sessions for each virtual object and each session contained a set of 5 trials for each type of manipulation task performed. All the manipulation tasks were executed with each trial starting with 5 seconds

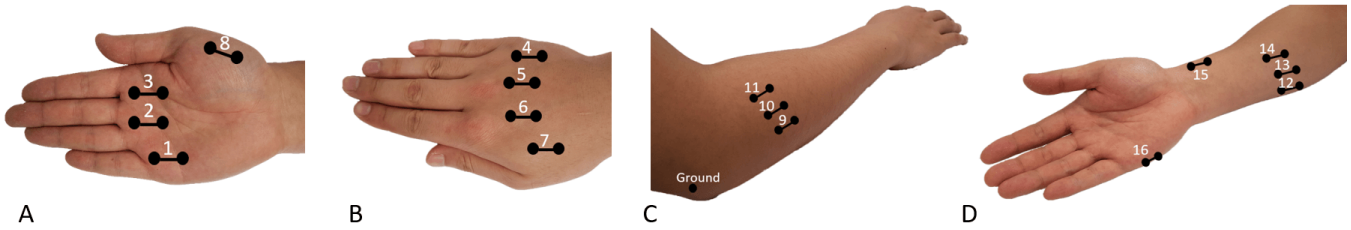

Fig. 5. EMG electrodes placement positions for a right hand dominant subject. The double dot with the connected line represents a bipolar pair of EMG electrodes distanced about 2 cm apart. Each electrode measures the myoelectric activations of certain muscles and is placed as follows: electrodes 1, 2, and 3 are placed on the Lumbrical muscles, electrodes 4, 5, 6, and 7 are placed on the Interossei muscles, electrode 8 is placed on the Opponens Pollicis muscle, electrodes 9, 10, and 11 are placed on the Extensor Digitorum muscle site, electrodes 12, 13, and 14 are placed on the Flexor Digitorum muscle site, electrode 15 is placed on the Abductor Pollicis Longus muscle and finally electrode 16 is placed on the Extensor Digiti Minimi muscle. The ground electrode is represented with a single dot and is placed near the elbow where muscular activity is minimal.

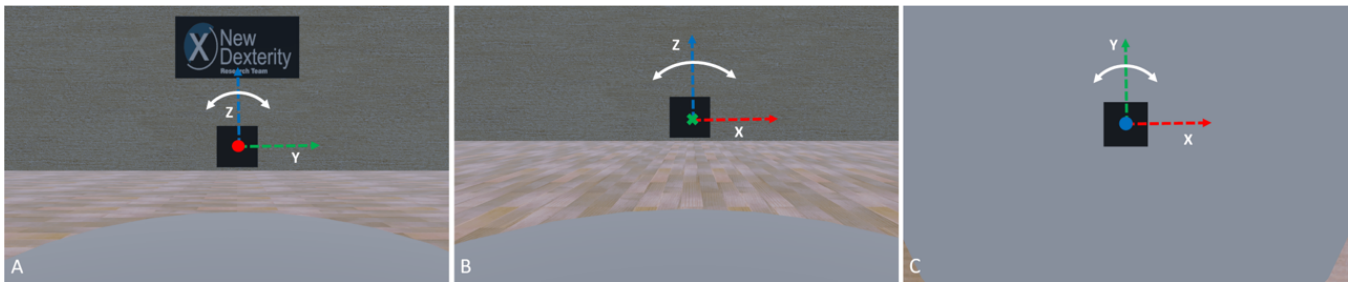

Fig. 6. Visualization of the pitch (subfigure A), roll (subfigure B), and yaw (subfigure C) manipulation motions performed during the experiments. Each axis is color coded and a colored 'circle' at the origin indicates that the positive direction of that axis is pointing orthogonally out of the page, while a colored 'X' at the origin indicates that it is pointing into the page. The white colored arrows show the direction of the motion about the out of plane axis.

of initial rest period followed by 15 repetitions of the manipulation motion. During rest period the participating subjects were required to hold the object stationary and get ready to execute the manipulation tasks. To minimize muscle fatigue, the subjects were given time to rest (approximately 30 s) between different trials, while a rest period of approximately 5 min between sessions was used. Additional rest time was provided in case the subjects experienced fatigue. The in-hand manipulation tasks executed during the experiments were pitch, roll, and yaw. Fig. 6 shows a visualization of each manipulation task performed, and these are as follows:

- Pitch: a coordinated movement of the fingers that results in a motion of the object along the x-axis
- Roll: a coordinated movement of the fingers that results in a motion of the object along the y-axis
- Yaw: a coordinated movement of the fingers that results in a motion of the object along the z-axis

III. Methods

A. EMG Feature Extraction

After acquiring the EMG signals, time domain (TD) features were extracted. To extract these features, a sliding window of 200 ms with a stride of 10 ms was selected. The size and the stride of the sliding window were carefully selected and configured to achieve the best possible performance for the decoding model. The window size should be as large as possible to avoid high biases and variances but not too large due to real-time constraints [22]. Three different TD features were extracted from each EMG channel, namely, Root Mean Square Value (RMS) [23], Waveform Length (WL) and Zero Crossings (ZC) [24], [25]. Further details regarding the extracted features can be found in [18].

B. Intention Decoding Scheme

The decoding of the user intentions while interacting with a virtual environment was formulated as a regression problem that maps the features extracted from the myoelectric activations to the motion of the virtual object. To do this, the Random Forests (RF) based regression methodology was selected. RF is an ensemble of decision trees proposed by Tin Kam Ho of Bell Labs [26]. A key feature of RF is the inherent ability of the method to calculate the feature variable importances, leading to better feature selection and improved accuracy (see [18] for details).

C. Learning Framework

In this study, we decode the motion of the object which is manipulated by the subject in the virtual world without any haptic feedback. To do this, the subjects performed the grasping and manipulation gestures in the virtual world, which were visualized using a HTC Vive VR headset, while the hand gestures were tracked with a glove equipped with six magnetic motion capture sensors. The myoelectric activations from the forearms and hands of the subjects were also acquired during these experiments. Time domain

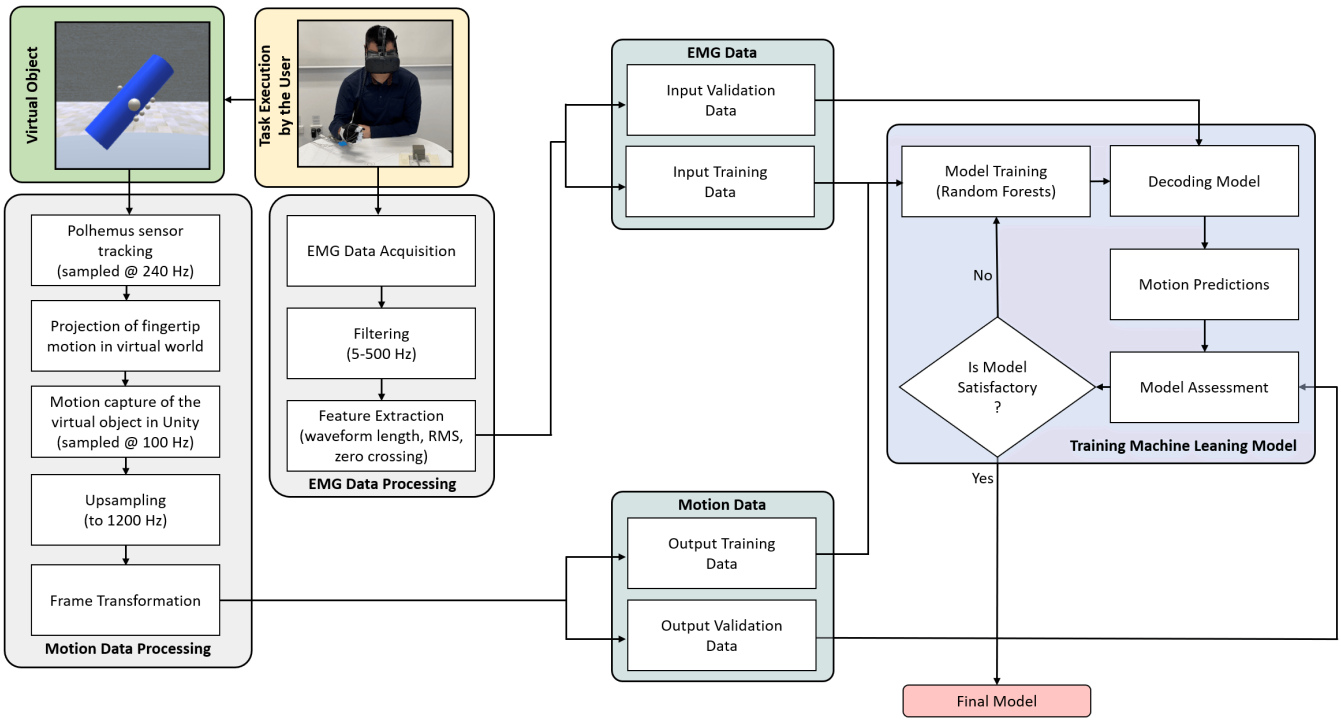

Fig. 7. Block diagram of the proposed EMG-based object motion decoding scheme in the virtual world. The subjects participating in the experiments executed dexterous manipulation motions with virtual objects. The EMG signals acquired from the muscles of the forearm and hand during object manipulation were filtered and time domain features were extracted. To collect the object motion data the fingertips of the subjects were tracked using a magnetic motion capture system and were projected into the virtual world to facilitate interaction with virtual objects. The motions of the virtual objects were recorded and the recordings were upsampled. Both the processed EMG and object motion readings were compiled into training and validation sets. The training sets were used as input to train the decoding models using the RF based learning scheme. The validation sets were used to assess the performance of the models by ensuring that the predicted motions of the virtual objects closely follow the true motions of the virtual objects. When the performance of the trained model was unsatisfactory, the model was retrained until the motion predictions were adequately accurate (using different RF parameters).

features were extracted from these EMG signals. The data of the features extracted was then compiled into two sets, one for training motion decoding models and the other to test their performance. The hyper-parameters of the framework (e.g. window size, window stride, RF parameters etc.) were tuned using an iterative training process that guarantees a satisfactory performance of the decoding model. Fig. 7 shows the EMG based learning framework utilized in this study. The final results present the average performance of the trained models over the 5 rounds of cross validation. To study the performance of the motion decoding models for different muscle regions, decoding models were trained for three different muscle groups consisting of: i) all the muscles of the forearm and the hand, ii) muscles of only the forearm, and iii) muscles of only the hand.

IV. Results

In this section, we present the average performance of the trained motion decoding models, calculated using a 5-fold cross validation process. We also present the importance of the muscles while decoding the manipulation motion on different objects. Pearson correlation coefficient and the percentage of the Normalized Mean Square Error (NMSE) for accuracy were used to compare the predicted object motion with the actual object motion. The NMSE value is defined as follows:

$$NMSE(\%) = 100 * \left(1 - \frac{||x_r - x_p||^2}{||x_r - mean(x_r)||^2}\right)(\%) \quad (1)$$

where, x_r is the actual reference motion and x_p refers to the predicted motion.

Table I shows the percentages of correlation and accuracy of the decoded motions for all the objects. It can be seen that the correlation of the decoded motion with the actual motion was as high as $\sim 92\%$, while the accuracy was as high as $\sim 83\%$. Fig. 8 shows the muscle importances while decoding each motion for each object, which were calculated using the RF methodology. The muscle importance values are normalized using the most important muscle for each subject. It can be noted that different subjects have higher importances for different muscle groups while executing the same motion on the same objects, suggesting that different subjects employ different task execution strategies for the same tasks. Another observation is that the importances of the hand muscles were higher than the importances of the forearm muscles for decoding the object motions. Table II shows the correlations and accuracies of the motion decoding models trained using only the muscles of the forearm, while Table III shows the correlations and accuracies of the motion decoding models trained using only the hand muscles. It is evident that a better performance of the decoding models can

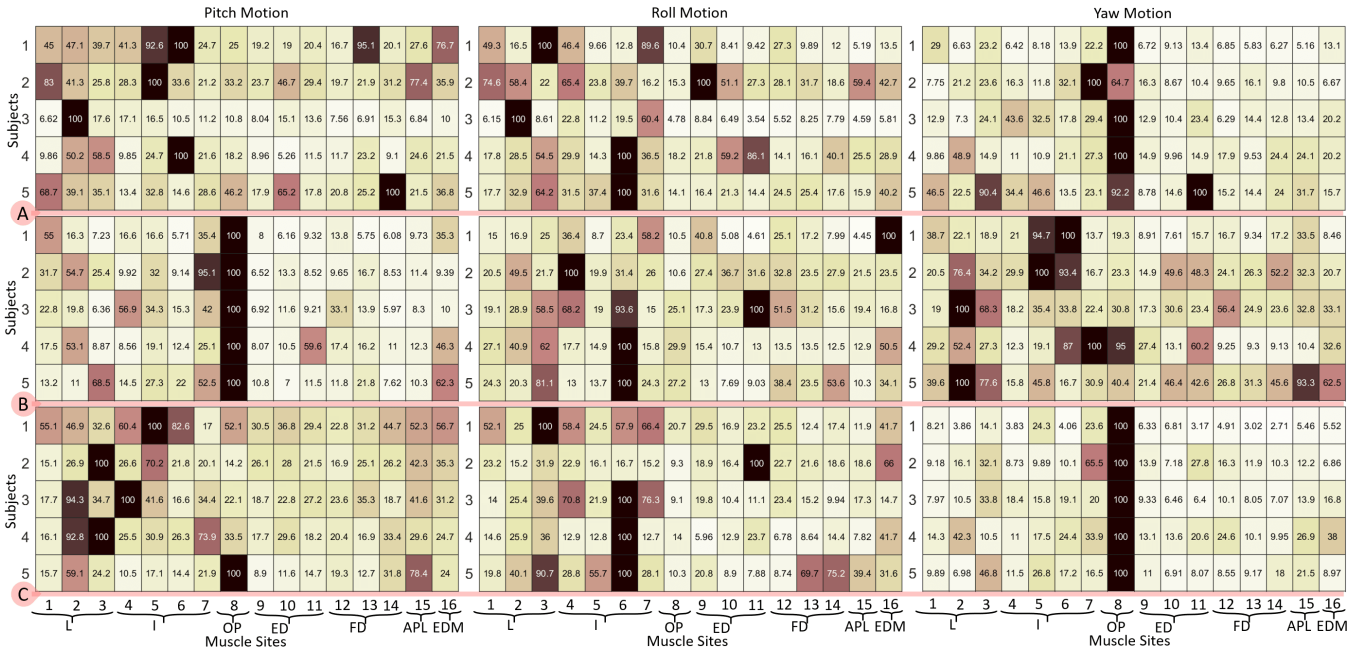

Fig. 8. Comparison of muscle importances for the motions performed on each of the objects. Subfigure A) presents muscle importances for the pitch, roll, and yaw (left to right) motions for the cube, while subfigure B) presents the same for cylinder, and subfigure C) for sphere. In x-axis, the various letters represent different muscle groups. More precisely, L represents Lumbricals, I represents Interossei, OP represents Opponens Pollicis, ED represents Extensor Digitorum, FD represents Flexor Digitorum, APL represents Abductor Pollicis Longus, and EDM represents Extensor Digiti Minimi.

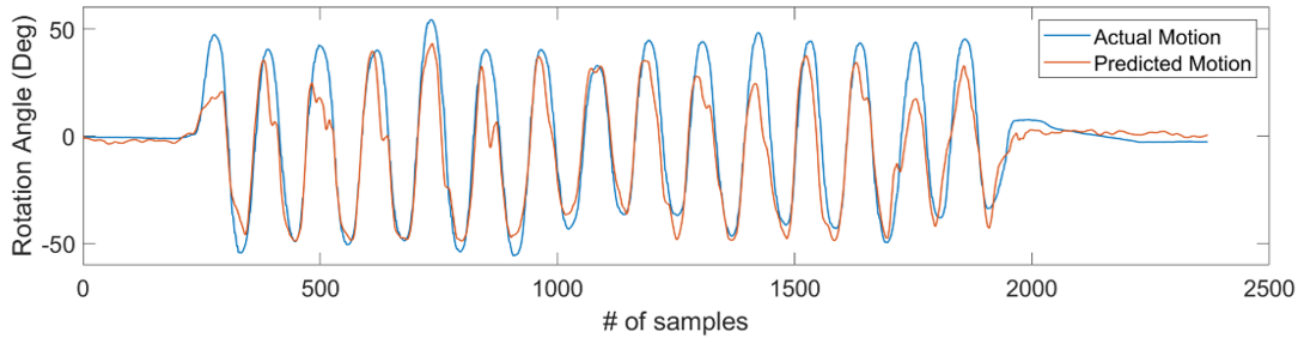

Fig. 9. Comparison of actual (blue) vs predicted (red) virtual object motion. The virtual object motion was decoded using the EMG signals of a subject.

be achieved if the models are trained using the myoelectric activations of the muscles of the hand. Fig. 9 shows an example of estimated virtual object trajectories. The actual virtual object motion (blue line) is compared with the decoded virtual object motion (red line) that is based on the human myoelectric activations.

V. Conclusion

In this study, we presented an EMG based learning framework for decoding the motion of a virtual object which is manipulated in a VR world without any haptic feedback. To do this, the subjects performed a series of manipulation experiments in a VR world visualized using a HTC Vive VR headset, while the hand gestures were tracked with a dataglove equipped with six magnetic motion capture sensors. The myoelectric activations from the muscles of the forearms and the hands of the subjects were also acquired during the experiments. Time domain features were extracted from the acquired EMG signals. The data of the features extracted was then divided into two sets, one for training and the other for validation. An iterative training and validation procedure was created to optimize the hyper-parameters of the framework (e.g., window size, window stride, RF parameters etc.).

From the results it can be concluded that it is feasible to decode motions of an object being manipulated in a virtual environment despite the lack haptic feedback and without considering other dynamic phenomena like friction and contact rolling and slipping. The correlations between the decoded and the actual motions were as high as $\sim$ 92%, while the model accuracies were up to $\sim$ 83% when trained using all the muscles. When trained using only the forearm EMG signals, the decoding performance was reduced considerably, while models trained only on the hand muscle activations performed similarly to the models trained with all the EMG signals from all the muscles. Thus, the performance of decoding models can be improved by using

TABLE I

CORRELATION (C) AND ACCURACY (A) FOR THE DECODING MODELS TRAINED ON THE MUSCLES OF BOTH FOREARM AND THE HAND. ALL THE REPORTED VALUES ARE IN PERCENTAGE.

Subject	Object	Motion					
		Roll		Pitch		Yaw	
		C	A	C	A	C	A
1	Cube	86.39	72.60	89.06	74.90	82.49	63.65
	Cylinder	80.88	56.02	91.05	78.61	83.36	61.13
	Sphere	77.56	48.73	73.75	48.50	90.61	81.51
2	Cube	76.80	56.94	70.35	37.76	81.85	66.17
	Cylinder	79.99	56.00	78.16	50.68	65.00	36.74
	Sphere	58.03	25.14	77.35	49.86	70.70	38.45
3	Cube	83.58	60.40	79.50	55.87	83.39	67.53
	Cylinder	71.95	50.23	78.09	54.77	28.06	5.29
	Sphere	79.67	53.92	67.96	39.62	83.01	66.77
4	Cube	81.12	62.05	85.09	71.10	80.20	60.64
	Cylinder	79.00	61.64	87.86	71.59	76.04	54.98
	Sphere	73.51	53.76	73.56	38.14	80.26	60.88
5	Cube	81.07	59.02	84.84	65.91	88.23	77.28
	Cylinder	82.84	66.31	89.95	79.73	80.56	57.13
	Sphere	82.12	65.84	83.70	65.74	92.73	83.74

the myoelectric activations of the hand and palm muscles. This suggests that muscle-computer interfaces based on hand muscles can be developed to facilitate an efficient, immersive interaction with virtual reality systems.

REFERENCES

[1] M. Ma and H. Zheng, "Virtual reality and serious games in healthcare," in *Advanced computational intelligence paradigms in healthcare 6. Virtual reality in psychotherapy, rehabilitation, and assessment*. Springer, 2011, pp. 169–192.

[2] M. Morehead, Q. Jones, J. Blatt, P. Holcomb, J. Schultz, T. DeFanti, M. Ellisman, G. Doretto, and G. A. Spirou, "Poster: Braintrek-an immersive environment for investigating neuronal tissue," in *2014 IEEE Symposium on 3D User Interfaces (3DUI)*, 2014, pp. 157–158.

[3] C. Moro, Z. Štromberga, A. Raikos, and A. Stirling, "The effectiveness of virtual and augmented reality in health sciences and medical anatomy," *Anatomical sciences education*, vol. 10, no. 6, pp. 549–559, 2017.

[4] A. Alzayat, M. Hancock, and M. A. Nacenta, "Quantitative measurement of tool embodiment for virtual reality input alternatives," in *Proceedings of the 2019 CHI Conference on Human Factors in Computing Systems*, 2019, pp. 1–11.

[5] K. A. Farry, I. D. Walker, and R. G. Baraniuk, "Myoelectric teleoperation of a complex robotic hand," *IEEE Transactions on Robotics and Automation*, vol. 12, no. 5, pp. 775–788, 1996.

[6] T. S. Saponas, D. S. Tan, D. Morris, R. Balakrishnan, J. Turner, and J. A. Landay, "Enabling always-available input with muscle-computer interfaces," in *Proceedings of the 22nd annual ACM symposium on User interface software and technology*, 2009, pp. 167–176.

[7] T. S. Saponas, D. S. Tan, D. Morris, and R. Balakrishnan, "Demonstrating the feasibility of using forearm electromyography for muscle-computer interfaces," in *Proceedings of the SIGCHI Conference on Human Factors in Computing Systems*, 2008, pp. 515–524.

[8] P. K. Artemiadis and K. J. Kyriakopoulos, "EMG-based teleoperation of a robot arm using low-dimensional representation," in *2007 IEEE/RSJ International Conference on Intelligent Robots and Systems*, 2007, pp. 489–495.

TABLE II

CORRELATION (C) AND ACCURACY (A) FOR THE DECODING MODELS TRAINED ON THE MUSCLES OF FOREARM ONLY. ALL THE REPORTED VALUES ARE IN PERCENTAGE.

Subject	Object	Motion					
		Roll		Pitch		Yaw	
		C	A	C	A	C	A
1	Cube	56.44	31.86	71.50	46.14	68.96	41.26
	Cylinder	5.10	0.00	59.22	31.83	44.02	2.47
	Sphere	28.83	7.26	35.93	0.96	62.43	38.17
2	Cube	64.60	40.93	57.69	26.37	60.60	29.97
	Cylinder	76.04	51.82	56.76	31.52	61.18	26.45
	Sphere	26.68	0.00	36.21	0.00	51.12	12.64
3	Cube	21.35	0.00	39.80	14.12	61.56	36.49
	Cylinder	55.40	29.71	55.74	15.17	3.79	0.00
	Sphere	22.16	2.95	49.93	20.69	32.85	8.12
4	Cube	76.92	56.18	30.33	7.10	52.73	23.90
	Cylinder	40.54	15.07	86.04	71.35	58.74	32.57
	Sphere	47.53	20.51	47.57	11.31	57.85	31.33
5	Cube	33.81	10.89	43.89	18.62	75.68	56.88
	Cylinder	38.34	14.11	80.28	61.69	42.70	8.28
	Sphere	66.23	41.83	68.88	44.45	83.73	68.77

TABLE III

CORRELATION (C) AND ACCURACY (A) FOR THE DECODING MODELS TRAINED ON THE MUSCLES OF HAND ONLY. ALL THE REPORTED VALUES ARE IN PERCENTAGE.

Subject	Object	Motion					
		Roll		Pitch		Yaw	
		C	A	C	A	C	A
1	Cube	81.94	65.40	83.52	65.53	81.72	62.41
	Cylinder	82.49	59.76	91.17	80.54	85.17	66.11
	Sphere	72.61	52.34	76.09	52.16	89.27	79.58
2	Cube	69.03	43.10	59.45	30.00	76.00	55.85
	Cylinder	78.55	54.11	78.97	54.47	47.62	18.96
	Sphere	11.82	0.00	76.99	54.52	71.36	39.77
3	Cube	85.93	71.73	80.95	59.89	83.52	68.64
	Cylinder	72.84	51.27	76.28	53.26	24.91	4.64
	Sphere	76.71	51.67	50.66	24.41	82.52	66.32
4	Cube	71.76	50.14	86.40	73.52	80.51	60.78
	Cylinder	79.18	62.27	79.16	59.60	79.55	58.58
	Sphere	73.53	52.77	76.30	52.19	79.75	61.35
5	Cube	81.34	61.20	79.17	59.33	83.84	69.16
	Cylinder	79.14	59.99	90.13	79.71	83.01	55.11
	Sphere	85.08	70.46	75.43	53.80	90.82	79.27

[9] M. V. Liarokapis, P. K. Artemiadis, P. T. Katsiaris, K. J. Kyriakopoulos, and E. S. Manolakos, "Learning human reach-to-grasp strategies: Towards EMG-based control of robotic arm-hand systems," in *IEEE International Conference on Robotics and Automation*, 2012, pp. 2287–2292.

[10] M. V. Liarokapis, P. K. Artemiadis, K. J. Kyriakopoulos, and E. S. Manolakos, "A learning scheme for reach to grasp movements: On EMG-based interfaces using task specific motion decoding models," *IEEE journal of biomedical and health informatics*, vol. 17, no. 5, pp. 915–921, 2013.

[11] D. Yang, J. Zhao, Y. Gu, X. Wang, N. Li, L. Jiang, H. Liu, H. Huang, and D. Zhao, "An anthropomorphic robot hand developed based on underactuated mechanism and controlled by EMG signals," *Journal of Bionic Engineering*, vol. 6, no. 3, pp. 255–263, 2009.

[12] M. Jiang, R. Wang, J. Wang, and D. Jin, "A method of recognizing finger motion using wavelet transform of surface EMG signal," in *Engineering in Medicine and Biology Society, 2005. IEEE-EMBS 2005. 27th Annual International Conference of the*, 2006, pp. 2672–2674.

[13] A. Dwivedi, G. Gorjup, Y. Kwon, and M. Liarokapis, "Combining electromyography and fiducial marker based tracking for intuitive telemanipulation with a robot arm hand system," in *2019 28th IEEE International Conference on Robot and Human Interactive Communication (RO-MAN)*, 2019, pp. 1–6.

[14] X. Zhang, X. Chen, W. Wang, J. Yang, V. Lantz, and K. Wang, "Hand gesture recognition and virtual game control based on 3D accelerometer and EMG sensors," in *Proceedings of the 14th international conference on Intelligent user interfaces*, 2009, pp. 401–406.

[15] D. J. Berger and A. d'Avella, "Towards a myoelectrically controlled virtual reality interface for synergy-based stroke rehabilitation," in *Converging Clinical and Engineering Research on Neurorehabilitation II*. Springer, 2017, pp. 965–969.

[16] A. Dwivedi, Y. Kwon, A. J. McDaid, and M. Liarokapis, "EMG based decoding of object motion in dexterous, in-hand manipulation tasks," in *7th IEEE RAS EMBS International Conference on Biomedical Robotics and Biomechatronics (BioRob)*, 2018.

[17] Y. Kwon, A. Dwivedi, A. J. McDaid, and M. Liarokapis, "On muscle selection for EMG based decoding of dexterous, in-hand manipulation motions," in *40th Annual International Conference of the IEEE Engineering in Medicine and Biology Society (EMBC)*, 2018.

[18] A. Dwivedi, Y. Kwon, A. McDaid, and M. Liarokapis, "A learning scheme for EMG based decoding of dexterous, in-hand manipulation motions." *IEEE Transactions on Neural Systems and Rehabilitation Engineering, Engineering in Medicine and Biology Society*, 2019.

[19] A. Dwivedi, J. Lara, L. K. Cheng, N. Paskaranandavadivel, and M. Liarokapis, "High-Density Electromyography Based Control of Robotic Devices: On the Execution of Dexterous Manipulation Tasks," in *IEEE International Conference on Robotics and Automation, ICRA*, 2020.

[20] B. Calli, A. Walsman, A. Singh, S. Srinivasa, P. Abbeel, and A. M. Dollar, "Benchmarking in manipulation research: Using the Yale-CMU-Berkeley object and model set," *IEEE Robotics & Automation Magazine*, vol. 22, no. 3, pp. 36–52, 2015.

[21] E. Todorov, T. Erez, and Y. Tassa, "Mujoco: A physics engine for model-based control," in *2012 IEEE/RSJ International Conference on Intelligent Robots and Systems*, 2012, pp. 5026–5033.

[22] M. A. Oskoei and H. Hu, "Myoelectric control systems: A survey," *Biomedical Signal Processing and Control, Elsevier*, vol. 2, no. 4, pp. 275–294, 2007.

[23] University of Guelph, "EMG Signals." [Online]. Available: http://www.soe.uoguelph.ca/webfiles/mleuniss/Biomechanics/EMG.html

[24] B. Hudgins, P. Parker, and R. N. Scott, "A new strategy for multifunction myoelectric control," *IEEE Transactions on Biomedical Engineering*, vol. 40, no. 1, pp. 82–94, 1993.

[25] D. Tkach, H. Huang, and T. A. Kuiken, "Study of stability of time-domain features for electromyographic pattern recognition," *Journal of neuroengineering and rehabilitation, BioMed Central*, vol. 7, no. 1, p. 21, 2010.

[26] T. K. Ho, "Random decision forests," in *Proceedings of the third international conference on Document analysis and recognition*, vol. 1, 1995, pp. 278–282.